Available online at www.sciencedirect.com
ScienceDirect
Cement and Concrete Research 38 (2008) 477–486
Cement and Concrete Research

Tricalcium aluminate hydration in additivated systems. A crystallographic study by SR-XRPD

Marco Merlini [a],*, Gilberto Artioli [a], Tiziano Cerulli [b], Fiorenza Cella [b], Anna Bravo [b]

[a] Dipartimento di Scienze della Terra "Ardito Desio", Università degli Studi di Milano, via Botticelli, 23, I-20133 Milano, Italy
[b] Mapei S.p.A, Lab. Ricerca e sviluppo, Via Cafiero 22, I-20158 Milano, Italy

Received 8 August 2005; accepted 23 November 2007

Abstract

Synchrotron radiation X-ray powder diffraction has been used to monitor the evolution of ettringite in C3A–gypsum synthetic mixture and in commercial cement systems during the first hours of the hydration process. The hydration of the paste was achieved using a remote controlled system, in order to collect data as soon as water is added to the system. The use of full-profile Rietveld method during the analysis of the diffractograms collected allowed us to monitor the evolution of phases weight fraction. The rigorous measurement of the lattice parameters and of the diffraction peak shape proved to be very useful to obtain information on the structural evolution of ettringite and on the mean grain size of the crystal phases. Depending on the admixture added to the system, the precipitation of well crystalline ettringite takes some hours. During this "induction" period we observe a significant variation of *a* and *c* lattice parameter values for ettringite. In particular *a* increases from 11.8 Å to 11.24 Å, the value for pure ettringite. The *c* parameter decreases from 22 Å to 21.48 Å. The lattice parameter variation could be related to small crystallite size effect, but the large variation more likely reflects also crystallographic changes, such as defect re-organization during the nucleation and growth process or also changes in the SO_3 and H_2O content in the ettringite channel. Not surprisingly the amount and the grain dimensions of crystalline ettringite are affected by the chemistry of the system. We observed the same evolution trend during ettringite formation also in shrinkage-compensating commercial cements (composed by mixture of Ca–Al cements, Portland cement and bassanite), in which ettringite is the main hydrous phase present.

Keywords: Synchrotron radiation X-ray powder diffraction; Ettringite; Superplasticizer; Rietveld method

1. Introduction

Tricalcium aluminate, $Ca_3Al_2O_6$ (C3A) is one of the main crystalline phases of cements [1]. It plays a fundamental role in the early stages of hydration process of Ordinary Portland Cements (OPC) and Calcium Aluminate Cements (CAC). The reaction of C3A with water produces calcium aluminate hydrate, Afm-type phases according to the cement nomenclature, and the more thermodynamically stable hydrogarnet [1,2]. The hydration of C3A is a strongly exothermic reaction and if the kinetics is not controlled, the so called "flash-setting" of cement may occur with undesirable effect on the rheological properties of the hydrating paste [1]. In order to prevent this reaction in cements, Ca-sulphate is usually added to the clinker [3]. When sulphates are present, ettringite is the phase crystallising during the hydration of C3A and the reaction is less exothermic. It is known from XRD analyses that crystalline ettringite is present since the early stages of hydration of the C3A paste [4]. Moreover observations performed by scanning electron microscopy show that at the beginning of the process ettringite appears with a gel-like morphology. The characteristics of the ettringite gel are thought to play a fundamental role in controlling both the dissolution kinetics of the clinker phases and the formation of hydrates. Ettringite, also called Aft-type phase, $C3A \cdot 3CaSO_4 \cdot 32H_2O$, is trigonal (space group P31c)

---

* Corresponding author. Tel.: +39 02 5031 5574; fax: +39 02 5031 5597.
E-mail address: marco.merlini@unimi.it (M. Merlini).

0008-8846/$ - see front matter © 2007 Elsevier Ltd. All rights reserved.
doi:10.1016/j.cemconres.2007.11.011

and the crystal structure is composed of columns of alternately Ca–(O,OH) and Al–(O,OH) octahedra along the *c* direction [5]. The columns are connected by SO_4 groups and water molecules, located in fairly large channels running parallel to the columns. The frequent morphology of synthetic and natural ettringite crystals is that of a prismatic fine needles elongated along *c*. Ettringite is present in the first hours of OPC hydration indicating that C3A and C4AF (Ca_2AlFeO_5) are the most reactive phases in the early stages of the hydration process [1]. Ettringite is also the main hydrate phase (at least in the first hours) in many other cementitious materials, such as shrinkage-compensating OPC/CAC based formulates, expansive cements, sulphoaluminate cements, etc. There is a close relationship between ettringite characteristics (i.e. morphology) and the physical properties (rheology, mechanical strengths) of the hydrating cement paste. In our opinion the knowledge of the crystallographic details of ettringite and of the kinetics of its formation in cementitious system is crucial to understand the physical behavior of cement materials. The kinetics of cement hydration is often studied following the evolution of physical or chemical properties in time. In fact the rheology, the mechanical strengths and the composition of pore solution can be related to the chemical reactions taking place. Moreover the samples can be quenched with different techniques, such as freezing or treating the material with organic solvents, and then prepared for conventional analyses [1], such as X-ray diffraction, thermal analyses and electron microscopy. However it has not been yet clarified if and how these quenching procedures do modify the crystalline structures of the phases involved, so that in recent years in-situ experiments based on synchrotron radiation (SR) and neutron powder diffraction were performed in order to study fast reactions without altering the sample [4,6,7]. We performed in-situ SR X-ray powder diffraction (XRPD) at ESRF, Grenoble during the hydration of a mixture composed by pure tricalcium aluminate (C3A) and Ca-sulphates. The hydration was carried out with water and solutions of commercial superplasticizers. We investigated also the hydration process of shrinkage-compensating cements in which ettringite is the main hydrous phase, in order to quantify the evolution of ettringite during the first hours of hydration and possibly correlate the evolution with the ettringite evolution in model systems composed by pure C3A and gypsum. We here report the results of the analysis performed by the Rietveld method, including the quantitative analysis of the phases and the estimate of the amorphous gel content and composition.

2. Experimental section

2.1. Materials and methods

$Ca_3Al_2O_6$ (C3A) was prepared by mixing in the stoichiometric ratio pure reagent grade Al_2O_3 and $CaCO_3$. The mixture was heated 4 h in air at 1000 °C, then crushed, mixed, pelletised and heated 12 h in air at 1450 °C with intermediate grindings. The product being synthesised was analysed by laboratory X-ray powder diffraction and almost pure cubic C3A was detected. It was ground and sieved; for the hydration experiments the fraction smaller than 63 μm was used. The source of sulphates in the system was Ca-sulphate hemihydrate ($CaSO_4 \cdot 0.5H_2O$), obtained by the dehydration of gypsum. We studied also the hydration of shrinkage-compensating cements composed by mixture of Portland cements (30%), Calcium Aluminate cement (40%) and bassanite (30%). Ettringite is the only crystalline hydrous phase which forms in the first days of hydration. The reactivity of the systems with water was preliminary investigated by calorimetric methods and the hydration process was monitored by electron microscopy with an environmental scanning electron microscope equipped with a field emission gun source (Philips FEI XL30 ESEM-FEG). The operating conditions were an accelerating voltage of 10 kV and the sample was maintained at 6.0 Torr and 5 °C. In these working conditions free water is pumped away, while water saturated with salts or contained in the crystalline phases or in the gel-like structures is preserved.

The X-ray powder diffraction experiments were performed at the European Synchrotron Radiation Facility (ESRF), Grenoble at the beamlines BM16 (now transferred to ID31) and BM08 (GILDA). In the experiments carried out at BM16 (ambient temperature hydration experiments) the wavelength used was 0.35448 Å, calibrated against standard silicon NIST SRM 630b. The samples were contained in a 1 mm glass capillary and water or a solution containing additives were injected in the capillary by a remote controlled peristaltic pump. The water added to the clinker was calculated to be in the ratio 1:1. The X-ray beam dimension at the sample was approximately 1×2 mm. Powder diffraction spectra were collected in the angular range 0.5–15 °2Θ, corresponding to a d-spacing range of 20.0–0.70 Å. Each experiment lasted few hours and in order to achieve an appropriate compromise between counting statistics and time-resolution, the scan speed was decreased during the experiment from 1 to 0.2 °2Θ/min. The experiments performed at the Italian Beam Line BM08 GILDA (high temperature experiments) were isothermal runs at 40, 60 and 70 °C. The samples were heated with a hot gas blower and the powder spectra were collected with a translating image plate system (TIP) detector [8]. This experimental setup is particularly suited for the study of reaction kinetics, since it allows a continuous recording of the diffraction peaks. The wavelength used was 0.68888 Å calibrated against standard LaB6, NIST SRM 660c. The isothermal runs lasted 4 h and the time-resolution was 2 min. The angular range explored was 1–40 °2theta, corresponding to a d-spacing interval 19–1 Å.

All powder diffraction spectra were indexed and elaborated with the Rietveld method [9,10] using the GSAS software [11]. Rietveld method is a powerful technique for the analysis of multi-phases mixtures, such as cements and several authors use it to quantify clinker phases [12–15]. The Rietveld refinements were performed using structural models for the phases taken from Inorganic Crystal Structure Database (ICSD). The refined parameters were: the scale factors, 15 terms for the background, modelled with a Chebyschev polynomial, the lattice parameters, and the profile parameters, in particular two coefficients for the Lorentian contribution to the full width at half maximum (FWHM) of the diffraction peaks (LX and LY of the GSAS package) for the data collected at BM16 and an added Gaussian term (GW) for the spectra collected at BM08. The profile function used was a pseudo-Voigt convoluted with a function which takes into account the axial divergence [16]; this function allowed to achieve a better fit of the peaks especially at low angles. C3A acted as an internal standard for the zero angle correction, which was found to be within 0.06 centidegree for the runs performed at BM16.

3. Results and discussion

3.1. Electron microscopy

The morphological study of the hydration reaction products of C3A was performed by ESEM-FEG. In Fig. 1-a a picture of the hydrated paste taken after 10 min from the beginning of the hydration is reported. A few prismatic crystals can be detected. As can be seen in Fig. 1-b, after 15 h the hydration process is close to the end and there are well-formed hexagonal prismatic crystals of ettringite.

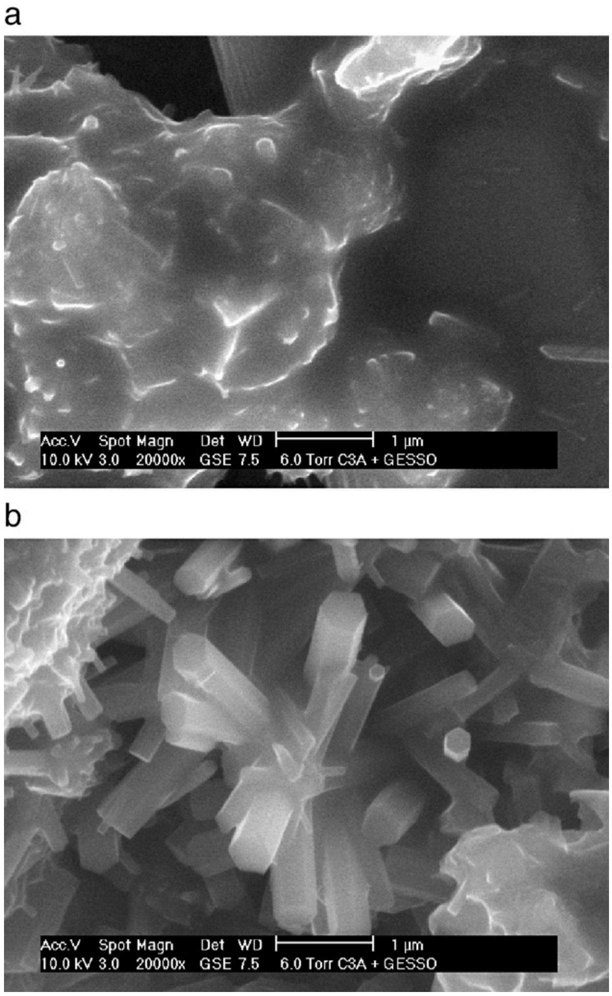

Fig. 1. a — ESEM image of hydration of a C3A/Gypsum paste taken after 10 min. b — ESEM image at the end of the hydration process of a C3A+gypsum paste.

3.2. Synchrotron radiation X-ray powder diffraction

3.2.1. The hydration of C3A in presence of sulphates and superplasticizers: quantitative analysis of the systems

Mixtures of C3A and bassanite in the proportion of about 70/30 by weight were hydrated: a) with an excess of water; b) with a solution 1.5% of commercial naphthalene sulphonated based plasticizer (NS); c) with a solution 1.5% of commercial poly-carboxylic-acid esthers based superplasticizer (PCAE). Just after water addition to the system the following chemical reactions occur:

$$CaSO_4 \cdot 0.5H_2O + H_2O \rightarrow CaSO_4 \cdot 2H_2O \qquad (1)$$

$$C3A + CaSO_4 \cdot 2H_2O \rightarrow C3A \cdot 3CaSO_4 \cdot 32H_2O \qquad (2)$$

(1) and (2) are global reactions, since ettringite precipitates from ions in solution or possibly ettringite nucleates and growths also from a sulpho-alluminate gel formed on the surface of clinker grains as soon as water is added to the system. Qualitative analysis of the powder pattern indicates that no crystalline phases other than C3A, bassanite, gypsum and ettringite were present during the experiments. In Fig. 2 X-ray diffraction patterns fitted with Rietveld method are reported. Fig. 2a refers to the pure clinker mixture, Fig. 2b is the powder pattern taken after 12 h from the beginning of hydration. Fig. 3 shows the weight fraction of the crystalline phases in the three experiments, obtained by Rietveld refinements. The errors calculated by the fitting procedure are quite small (0.1 wt.%). In order to assess the accuracy of the results, we estimated the errors averaging the results of the quantitative analysis performed on the dry mixtures (C3A and bassanite) before hydration (5 samples). The standard deviations calculated in this way are around 1.5 wt.% and this value seems to be more plausible. The first reaction that can be monitored is the dissolution of bassanite and gypsum formation. This reaction is very fast in the pure-water system, but it is much slower if plasticizers are present (Fig. 4). Moreover the kinetics is different depending on the plasticizer employed. In all the experiments ettringite forms immediately at the start of hydration, but its growth-rate is strongly affected by the type of admixture present in the system. At any given time in the system with NS the amount of crystalline ettringite formed is always greater than in the systems containing pure water or PCAE.

In order to correctly interpret the results of the quantitative analyses it must be taken into account that the sum of the crystalline phase mass fractions is constrained by the program to be equal to 1. If an amorphous phase is present, it cannot be quantified directly by diffraction, therefore the mass fractions of the crystalline phases are overestimated. In our case the ESEM observations confirm the presence of a gel phase, especially in the first stages of the process, and correspondingly the X-ray powder patterns show an increase of the background. In all the experiments the C3A content increase at the start can only be attributed to the formation of an amorphous phase. The amorphous content can be determined if the mass fraction of one

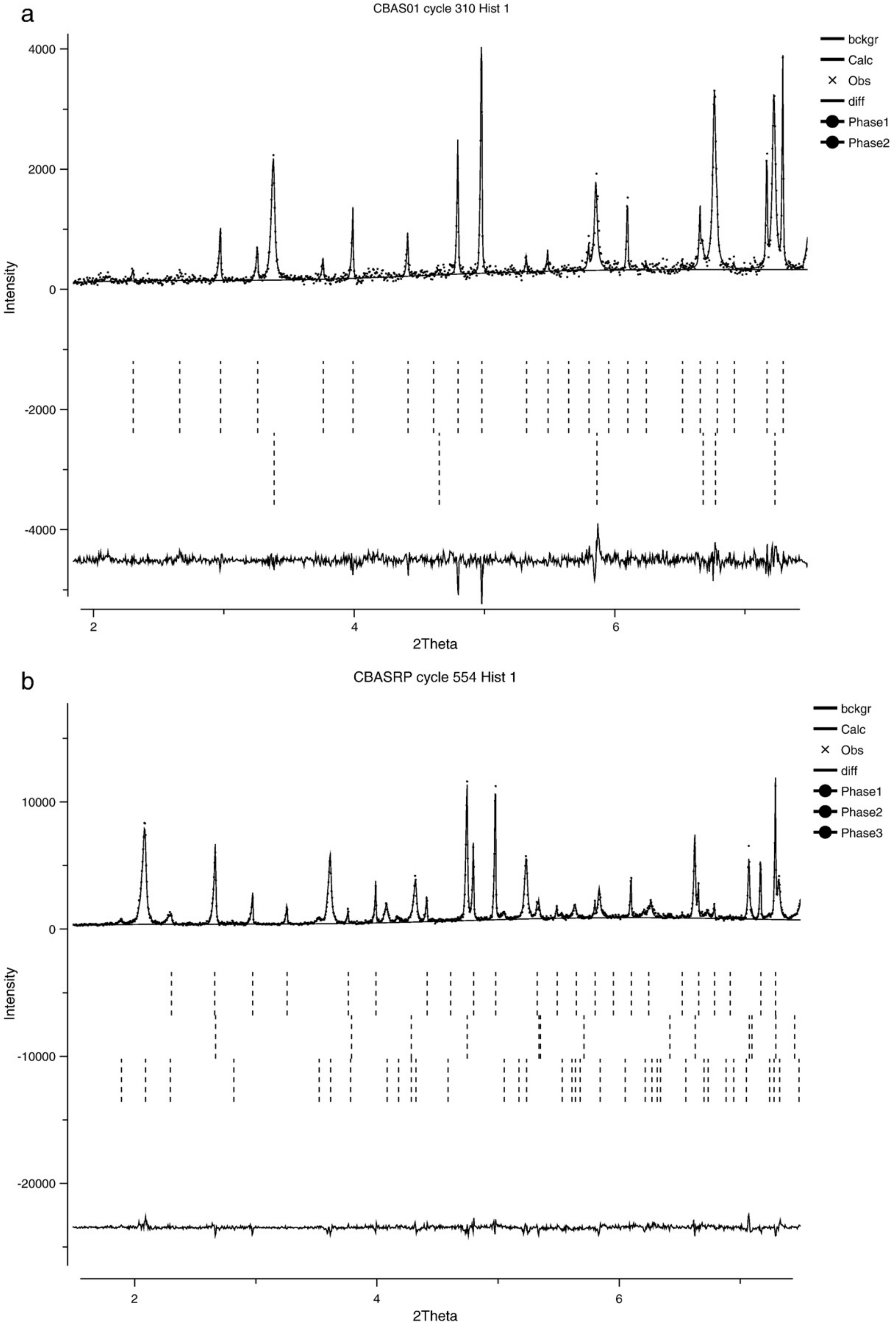
a
CBAS01 cycle 310 Hist 1
bckgr
Calc
× Obs
diff
Phase1
Phase2
Intensity
4000
2000
0
-2000
-4000
2
4
6
2Theta
b
CBASRP cycle 554 Hist 1
bckgr
Calc
× Obs
diff
Phase1
Phase2
Phase3
Intensity
10000
0
-10000
-20000
2
4
6
2Theta

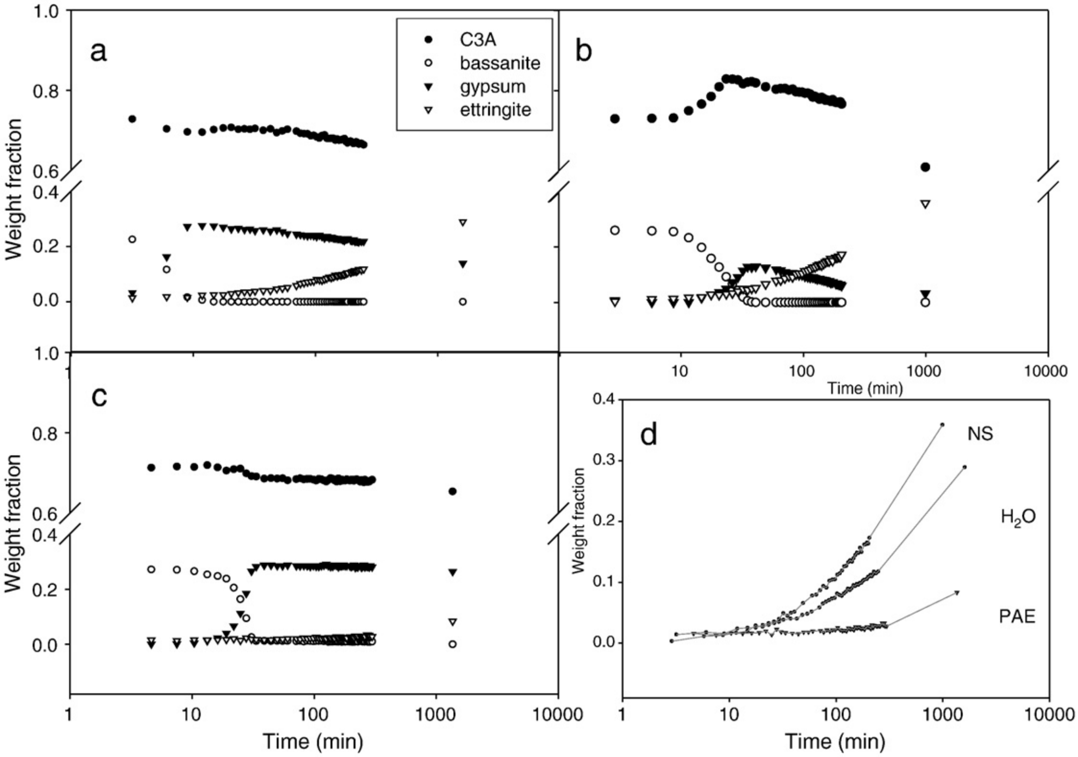

Fig. 3. Evolution of the crystalline phases in the different experiments: a) C3A–$CaSO_4$ paste hydrated with water; b) C3A–$CaSO_4$ paste hydrated with solution of NS polymers; c) C3A–$CaSO_4$ paste hydrated with solution of PAE polymers; d) the amount of crystalline ettringite in the different systems (see text for discussion).

phase is known [17]. With the assumption that the amount of material investigated by the X-ray beam doesn't change during the experiment and that no amorphous phase is present at the beginning of the process, the refined value of the scale factor of a given phase can be used to calculate the absolute amount of that phase, since the scale factor is proportional to its volume (and hence to the mass). Under this assumption the weight percent (W) of C3A in the ith diffractograms W_i is given by:

$$W_i = (S_i/S_0)\cdot W_0$$

W_0	known weight percentage
S_0	scale factor of C3A at the beginning, corresponding to W_0
S_i	scale factor of C3A at a given time

In this way we have a direct measurement of the C3A wt.%, which is independent from the weight percentage of the other phases. Therefore C3A can be used as internal standard during the hydration process and the amorphous content can be estimated. Because of the assumptions made, the estimation of amorphous content is quite accurate only if its quantity is greater than 3–4%, because slight variation in density of the paste, and hence the volume of material probed by the X-ray beam, could affect the accuracy of the results. In the case of hydration with NS the amount of the amorphous phase reach the values of 15% after 20 min (Fig. 5). On the contrary in the case of hydration with water or PCAE the amorphous content is instead in the range of a few units percent.

Assuming a pure composition for the crystalline phases, it is also possible to calculate the chemical composition of the crystalline fraction of the system in the different experiments. The results are reported in Fig. 6. In the system hydrated with NS, and to a lesser extent also in the system hydrated with water or PCAE, the sum of the crystalline phases does not balance the starting chemical composition, at least in the first stages of hydration. In particular we could observe a noticeable decrease in SO_3 content in the crystalline fraction of the system with respect to the starting value. This indirectly indicates that the amorphous phase is rich in SO_3. The enrichment in SO_3 content in the amorphous phase is particularly evident in the system hydrated with NS.

3.2.2. The hydration of C3A in presence of sulphates and superplasticizers: lattice and profile parameters refinements

Lattice and profile parameters of the crystalline phases were obtained by Rietveld refinements. The parameters for C3A were refined using a powder spectra collected from the pure phase

Fig. 2. a — X-ray powder diffraction of mixture of C3A – bassanite, fitted with Rietveld method. The observed, calculated and difference lines are reported. The ticks in the figure refer to the C3A and bassanite diffraction peaks position respectively. b — X-ray powder pattern of the mixture C3A–bassanite after 12 h of hydration. Bassanite is no more present. The ticks in the figure refer to C3A, gypsum and ettringite respectively.

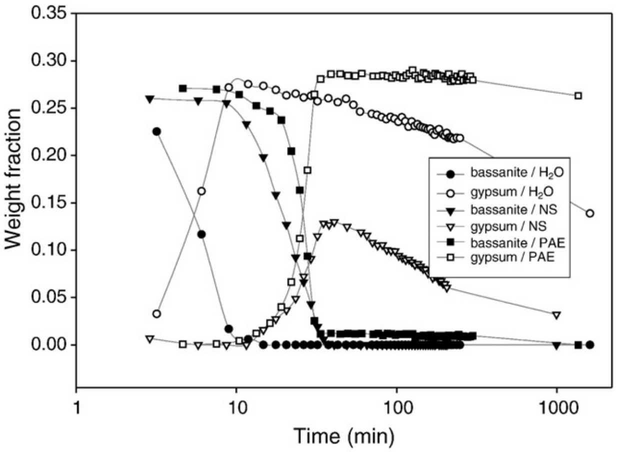

Fig. 4. Bassanite and gypsum weight fraction in the different experiments.

and the values obtained were kept constant in all the refinements. Fig. 7 is a plot of the lattice parameter of ettringite vs. time in the different experiments. In the case of hydration with pure water there is an increase of *a* and a decrease of *c* and they both converge to the ideal lattice parameters of pure ettringite in a few hours. The same trend is observed also in the presence of NS. In the presence of PCAE the variation of the lattice parameter is less pronounced. The increase of *a* with time during the crystallisation of ettringite was previously reported [4], and interpreted with a variable SO_3/OH (or H_2O) ratio in the structure. In fact pure hydroxyl-ettringite has a smaller molar volume. The hypotheses of a SO_3/H_2O variable ratio can account for the shrinkage in the *ab* plane at the beginning of hydration, but in order to explain also the greater dimension along *c* other structural features must be taken into account. Possible explanations for the variation of the *c* parameter, could be a partial substitution Ca^{2+}/Al^{3+} in the column or, more likely, the presence of OH groups substituting oxygen at the corners of the Al or Ca coordination polyhedra. The incorporation into the structure of additional water molecules and/or a rotation of SO_3 groups in the channels could also account for a slight variation of *c*. The profile parameter values can provide information about physical features of the phases; in particular the full width at half maximum (FWHM) can be related to the mean crystallite size. During the Rietveld refinement it was observed that the LY

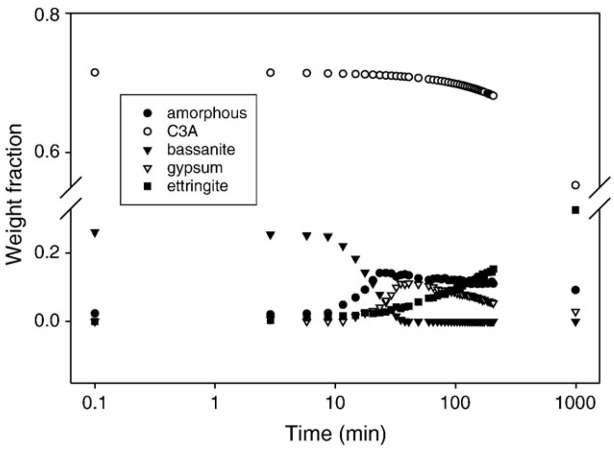

Fig. 5. Mass fraction recalculation including the amount of amorphous phase formed during the hydration process with NS admixtures.

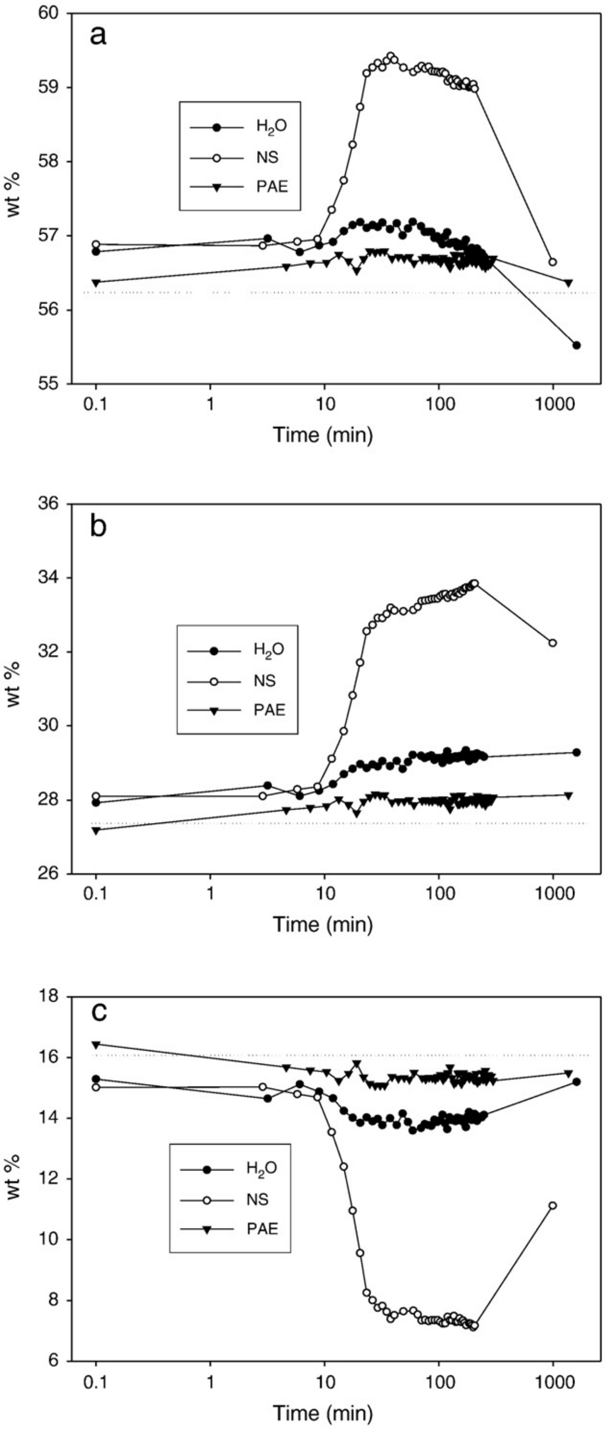

Fig. 6. Anhydrous chemical composition of the crystalline fraction of the systems studied calculated from quantitative analyses: a) CaO wt.%; b) Al_2O_3 wt.%; c) SO_3 wt.%. The dotted lines indicate the approximate starting composition. The decrease of SO_3 is noticeable in the crystalline portion of the system especially in the presence of NS polymers.

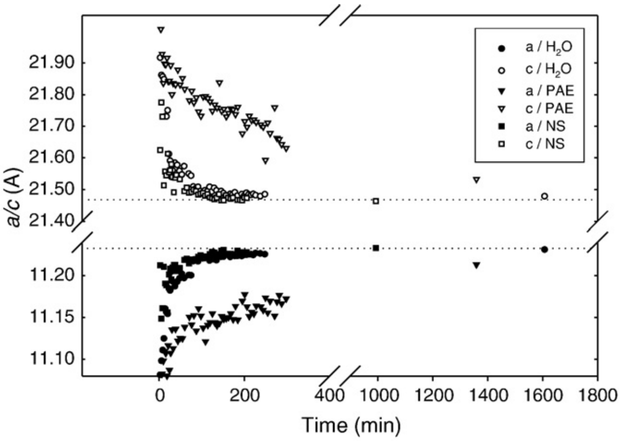

Fig. 7. *a* and *c* lattice parameter values of ettringite in the different experiments. The dotted lines indicate the lattice parameter values for stoichiometric pure ettringite.

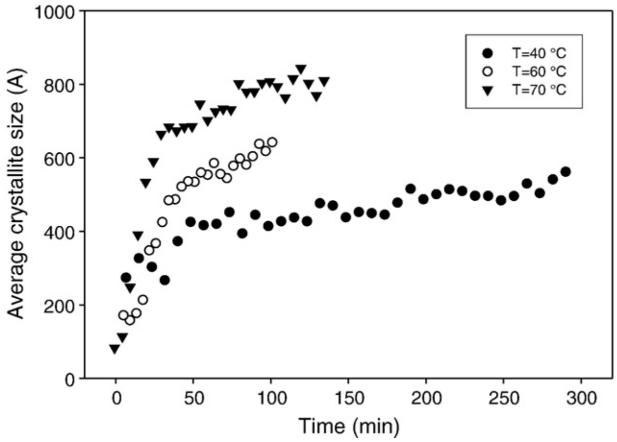

Fig. 9. Average crystallite size of ettringite estimated in experiments of hydration of C3A–gypsum mixture performed at 40, 60 and 70 °C.

coefficient of the Lorentzian function converged approximately to a constant value and LX varied as function of time, so that in the final refinement cycles LY was kept constant (fixed to the average refined values) and only LX was refined. Since the crystallite size produces a profile broadening with an angular dependence proportional to 1/cos*θ* [18], the refined values of LX can be related to the average grain size using the Scherrer equation. The instrumental contribution to the FWHM, which is very limited at the BM16 beamline, and the needle shape of the crystals, which can introduce a directional broadening of the diffraction peaks, were neglected. However the values obtained proved to be very useful to compare different experiments performed with the same experimental configuration and allowed to appreciate differences in the nucleation and growth mechanism depending on the chemical system and admixture used. The results are reported in Fig. 8. Similar data analyses were applied to the experiments performed at different temperatures at the Italian beam line (GILDA); the major difference arise from the larger instrumental contribution to the FWHM. A constant term for a Gaussian broadening of the peak shape (GW of the GSAS package) was then added in order to take into account the instrumental contribution. Fig. 9 is a plot of the average grain size as function of time for the three

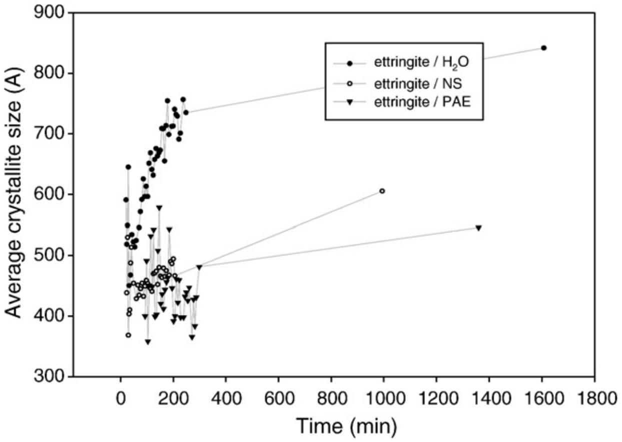

Fig. 8. Average crystallite size of ettringite estimated in the different experiments.

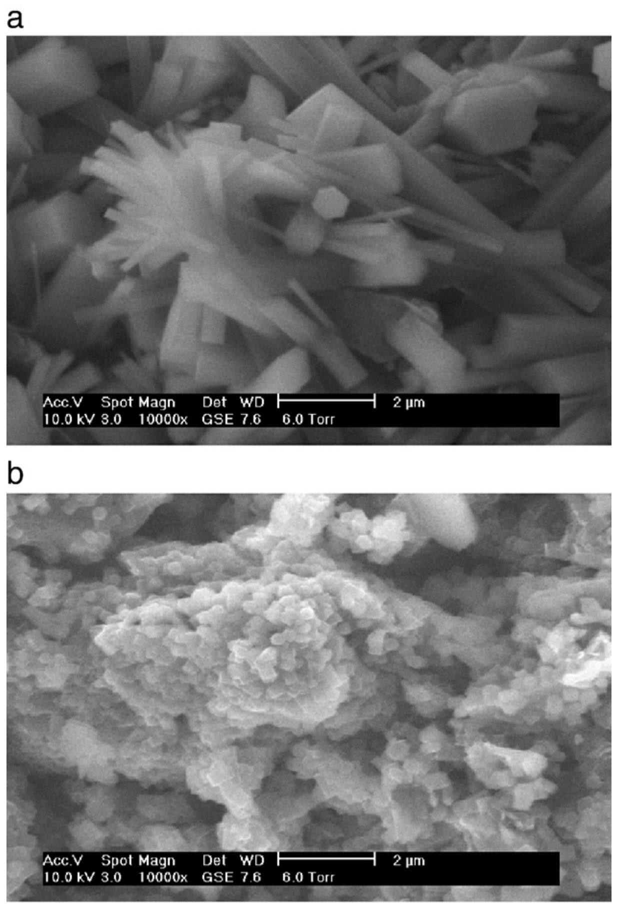

Fig. 10. a — ESEM image of ettringite morphology in high performance shrinkage-compensating cement. Picture taken after 8 h of hydration. b — ESEM image of ettringite morphology in low performance shrinkage-compensating cement. Picture taken after 8 h of hydration.

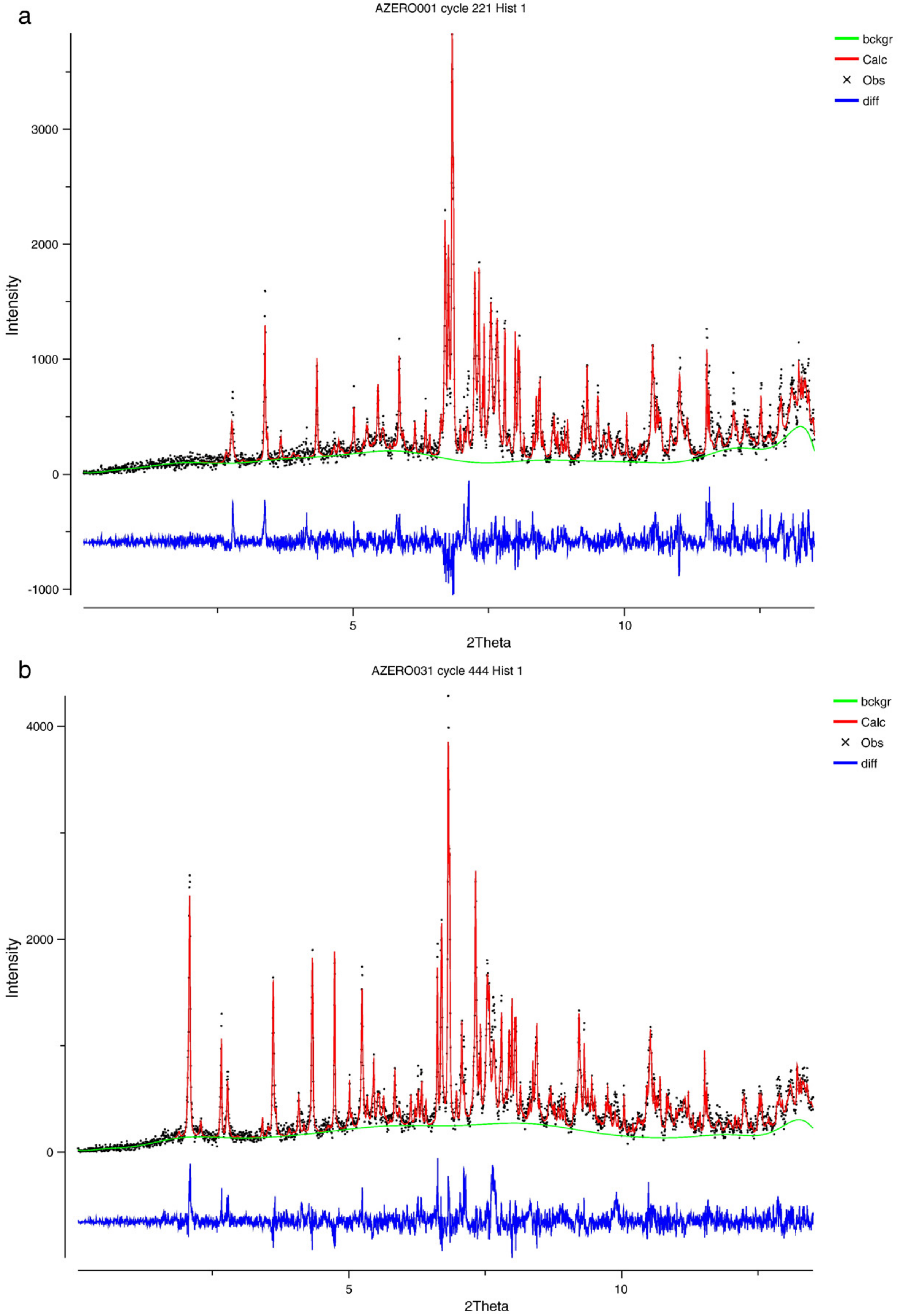
a
AZERO001 cycle 221 Hist 1
bckgr
Calc
× Obs
diff
Intensity
3000
2000
1000
0
-1000
5
10
2Theta
b
AZERO031 cycle 444 Hist 1
bckgr
Calc
× Obs
diff
Intensity
4000
2000
0
5
10
2Theta

isothermal experiments. This data indicate an increase of the grain size as function of the hydration temperature.

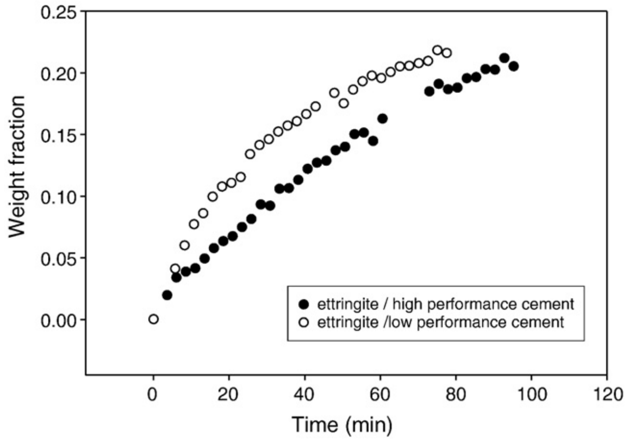

Fig. 12. Weight fraction of ettringite in shrinkage-compensating cements.

4. Ettringite evolution in shrinkage-compensating cements

Low shrinkage or shrinkage-compensating cements are high performance cements that make use of controlled expansive chemical reactions to compensate for drying shrinkage and minimize cracks due to internal stresses [19]. We investigated with SR-XRPD the phase evolution in two systems composed by mixture of OPC, CAC and bassanite. The two formulates studied have similar chemical and phase composition but they develop different physical properties, especially in the first hours. In particular the compressive strength of high performance cement reach 40 N/mm^2 after 24 h, while for low performance cement it is only half of it. ESEM images of the two hydrating pastes showed larger ettringite crystals, which develop higher mechanical strengths. Fig. 10 a and b compare the two cements after 8 h of hydration. A study performed on similar systems employing SR source is already reported [20]. The reported results, based on single peak fitting procedures, pointed out how in the first hours ettringite is the only hydrous phase present. Subsequently, after the total consumption of gypsum, Afm phases form, depending on the total amount of sulphate available in the system. We performed Rietveld refinements and two powder patterns collected before the hydration and after 2 h of hydration are reported in Fig. 11. The results of the quantitative analysis for ettringite are reported in Fig. 12. CA (CaOAl2O4) was the most abundant phase. Bassanite is 20% of the sample at the start, and completely disappears after 40 min. CA was consumed and ettringite was formed. The total amount of ettringite was quite comparable in the two systems. The only difference observed was the total amount of gypsum formed, which was slightly higher in the cement with lower performances. Refined lattice and profile parameters of ettringite indicate a different evolution of this phase with time in the two samples. The estimate of the average crystal size (Fig. 13) is in agreement with ESEM observations, indicating that in the paste having higher mechanical strengths the ettringite crystals are larger than in the other system. Lattice parameter values are plotted vs. time in Fig. 14. The increase of *a* and the decrease of *c* with time in the two systems, resemble the behavior of pure C3A hydrating systems. However while in the system with normal mechanical properties the evolution of ettringite to the standard crystalline structure is achieved within the first hour, in the system with lower mechanical properties this does not happen and the absolute value of lattice parameters are always smaller than the one of pure ettringite.

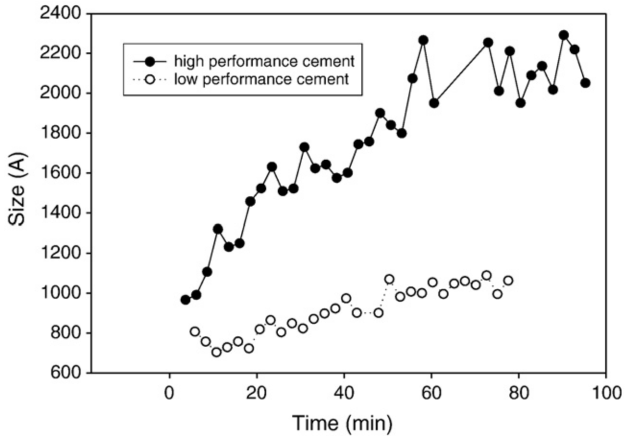

Fig. 13. Average crystallite size of ettringite in shrinkage-compensating cements.

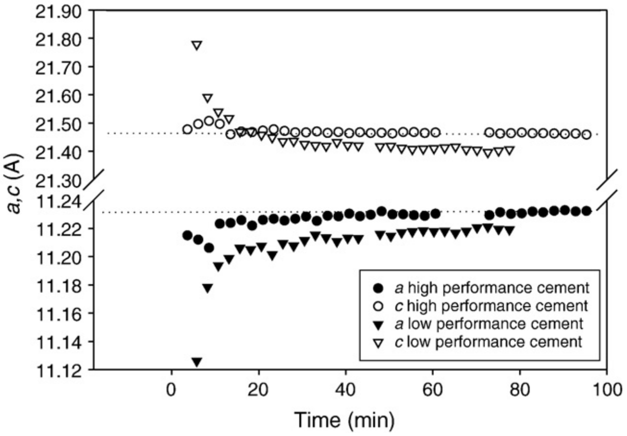

Fig. 14. *a* and *c* lattice parameter values of ettringite in shrinkage-compensating cements.

5. Conclusions

The use of synchrotron radiation X-ray powder diffraction proved to be very useful in the experimental study of cements. In fact the high brilliance of the source allowed to collect in few

Fig. 11. a — X-ray powder diffraction pattern of a low shrinkage cement, composed by a mixture of Portland cement, calcium aluminate cement and bassanite. The mineralogical composition of this cement is CA 40%, C3S 12%, C4AF 14%, C3A 9%, CaCO3 5% and bassanite 20%. b — X-ray powder diffraction pattern of a low shrinkage cement after 2 h of hydration. The first peak is the ettringite (100) peak.

minutes powder spectra with a good statistics suitable for Rietveld analysis, thus for a full kinetic study of the process. Furthermore, the extremely low instrumental contribution to the peak broadening allowed to extract reliable information from lattice and profile parameters also for phases present at very low concentrations, such as the forming hydrous phases in cements. As far as the pure C3A system is concerned, the total amount of crystalline ettringite in the systems with added superplasticizers can be either higher or lower than the one formed in pure water. The total amount of crystalline ettringite is possibly not the most crucial aspect in order to explain the physical properties of cement systems. When NS is used, a detectable amount of amorphous phase rich in sulphates is present, which is consistent with the hypothesis of formation of an organo-mineral phase [21]. The stability of this phase could reduce the actual sulphate availability for ettringite and monosulphate formation with respect to the theoretical amount of gypsum. However the most considerable result obtained concerns the crystallographic evolution of ettringite with time, as revealed by the change in the lattice parameters. This is an experimental indication that the chemical equilibria in the gel and in the solution evolve during the process. In the first stages of hydration it is possible that the structure has a different SO_3/H_2O ratio than stoichiometric pure ettringite. The studies performed on complex cement systems, in which the mechanical properties are mainly based on ettringite, evidenced that in the case of the low performance material (i.e. low mechanical strengths) ettringite needs longer times to reach structural stability.

Acknowledgements

We acknowledge the European Synchrotron Radiation Facility for the provision of synchrotron radiation beam time. We acknowledge in particular J. Wright and C. Meneghini for their assistance on BM16 and BM08. Davide Salvioni is acknowledged for the ESEM images. Monica Dapiaggi and Walter Tiano are acknowledged for their help during XRPD data collection.

References

[1] H.F.W. Taylor, Cement Chemistry, 2nd ed. Thomas Telford Publishing, London, 1997.
[2] E.M. Gartner, J.F. Young, D.A. Damidot, I. Jawed, Hydration of Portland Cement, in: J. Bensted, P. Barnes (Eds.), Structure and Performance of Cements, Spon Press, London, 2002.
[3] J. Bensted, Gypsum in Cements, in: J. Bensted, P. Barnes (Eds.), Structure and Performance of Cements, Spon Press, London, 2002.
[4] P. Barnes, et al., The Use of Synchrotron Sources in the Study of Cement Materials, in: J. Bensted, P. Barnes (Eds.), Structure and Performance of Cements, Spon Press, London, 2002.
[5] A.E. Moore, H.F.W. Taylor, Crystal structure of ettringite, Acta Crystallogr. B26 (1970) 386–393.
[6] S.M. Clark, P. Barnes, A comparison of laboratory, synchrotron and neutron diffraction for the real time study of cement hydration, Cem. Concr. Res. 25 (3) (1995) 639–646.
[7] M. Castellote, C. Alonso, C. Andrade, J. Campo, X. Turrillas, In situ hydration of Portland cement monitored by neutron diffraction, Appl. Phys. A Mater. Sci. Process. 74 (Suppl., Pt. 2) (2002) S1224–S1226.
[8] C. Meneghini, G. Artioli, A. Balerna, A.F. Gualtieri, P. Norby, S. Mobilio, Multipurpose imaging-plate camera for in situ powder XRD at the GILDA beamline, J. Synchrotron Radiat. 8 (2001) 1162–1166.
[9] H.M. Rietveld, A profile refinement method for nuclear and magnetic structures, J. Appl. Crystallogr. 2 (1969) 65–71.
[10] R.A. Young (Ed.), The Rietveld Method, Oxford University Press, 1993.
[11] A.C. Larson, R.B. Von Dreele, General Structure Analysis system (GSAS), Los Alamos National Laboratory Report LAUR, 1994, pp. 86–748.
[12] J.C. Taylor, Z. Rui, L-P. Aldridge, Full-profile Rietveld quantitative XRD analysis of Portland cement: standard XRD profiles for the major phase tricalcium silicate C3S, Powder Diffr. 8 (3) (1993) 138.
[13] F. Guirado, S. Gallí, S. Chinchón, Quantitative Rietveld analysis of aluminous cement clinker phases, Cem.Concr. Res. 30 (2000) 1023–1029.
[14] M. Castellote, X. Turrillas, C. Andrade, C. Alonso, A. Kvick, A. Terry, G. Vaughan, J. Campo, Synchrotron Radiation Diffraction Study of the microstructure changes in cement paste due to accelerated leaching by application of electrical fields, J. Am. Ceram. Soc. 85 (3) (2002) 631–635.
[15] A. G de la Torre, M.A. García, Rietveld Mineralogical Analysis of Portland Cements, in: F. Grieve, G. Owens (Eds.), Proceedings of the 11th International Congress on the Chemistry of the Cement (ICCC). Cement's Contribution to Development in the 21st Century, 2003, pp. 135–144.
[16] L.W. Finger, D.E. Cox, A.P. Jephcoat, A correction for powder diffraction peak asymmetry due to axial divergence, J. Appl. Crystallogr. 27 (1994) 892–900.
[17] D.L. Bish, S.A. Howard, Quantitative phase analysis using the Rietveld method, J. Appl. Crystallogr. 21 (1988) 86–91.
[18] B.E. Warren, X-ray Diffraction, Dover Publications, Inc., New York, 1969.
[19] P. Metha, G. Lensikoff, Hydration characteristics and properties of shrinkage-compensating cements, Proceedings of the 6th International Congress on the Chemistry of Cement, Stroyzdst, Moscow, vol. 3, 1976, pp. 89–115.
[20] C. Hevju, S. Hansen, Expansive properties of ettringite in a mixture of calcium aluminate cement, Portland cement and calcium sulphate hemihydrate, Cem. Concr. Res. 31 (2001) 257–261.
[21] V.S. Ramachandran, V.M. Malhotra, C. Jolicoeur, N. Spiratos, Superplasticizers: Properties and Applications in Concrete, CANMET publ., Ottawa, Canada, 1998.